Electronic Supplementary Information

Kinetics and mechanistic details of bulk ZnO dissolution using a thiol-imidazole system

Kristopher M. Koskela,[1] Stephen J. Quiton,[2] Shaama Mallikarjun Sharada,[1,2,*] Travis J. Williams,[1,3,*] and Richard L. Brutchey[1,*]

[1] Department of Chemistry, University of Southern California, Los Angeles, CA 90089, USA
[2] Mork Family Department of Chemical Engineering and Materials Science, University of Southern California, Los Angeles, CA 90089, USA
[3] Loker Hydrocarbon Institute, University of Southern California, Los Angeles, CA 90089, USA

*Email: ssharada@usc.edu, travisw@usc.edu, brutchey@usc.edu

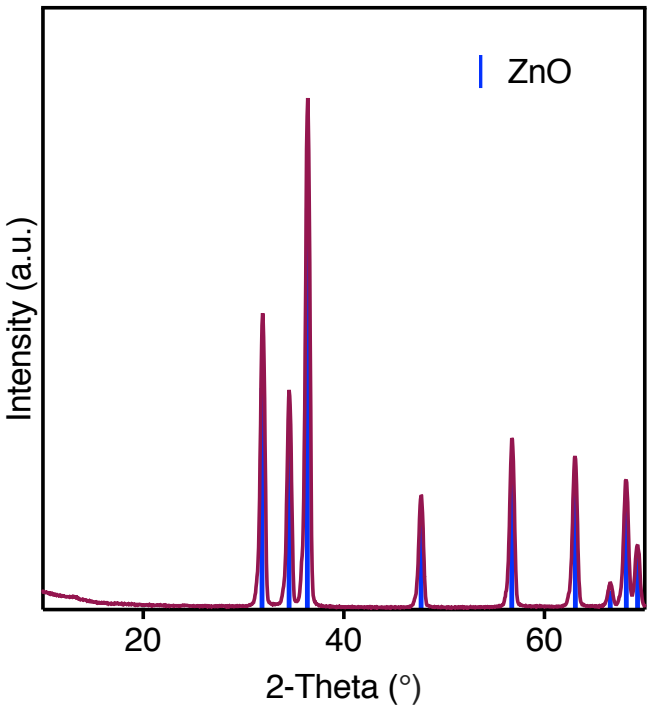

Fig. S1 Powder XRD pattern of polycrystalline ZnO powder starting material (99.99%, Alfa Aesar) indexed to the wurtzite crystal structure.

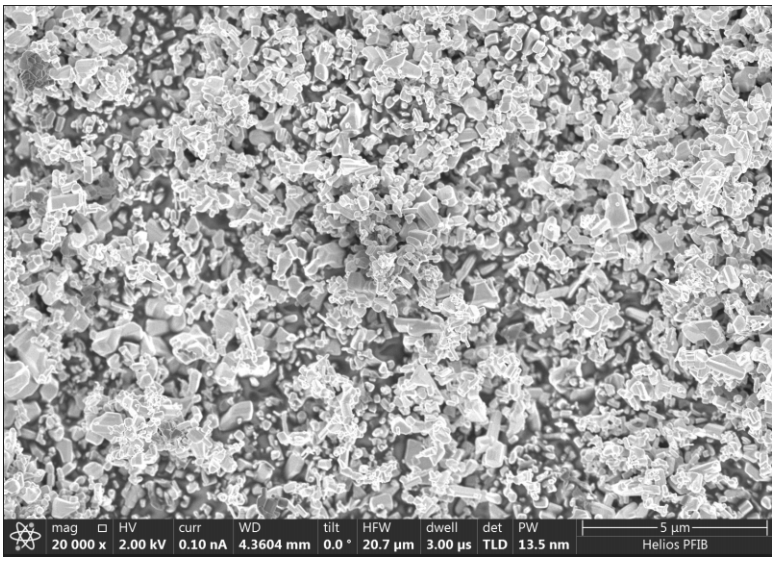

Fig. S2 SEM micrograph of polycrystalline ZnO powder starting material (99.99%, Alfa Aesar).

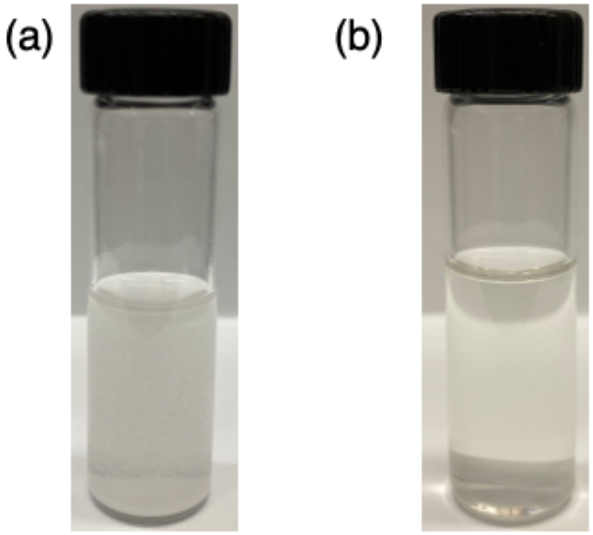

Fig. S3 Representative photographs of synthetic polycrystalline ZnO powder dissolution in MeIm and acetonitrile (a) before thiophenol addition and (b) after thiophenol addition and full dissolution.

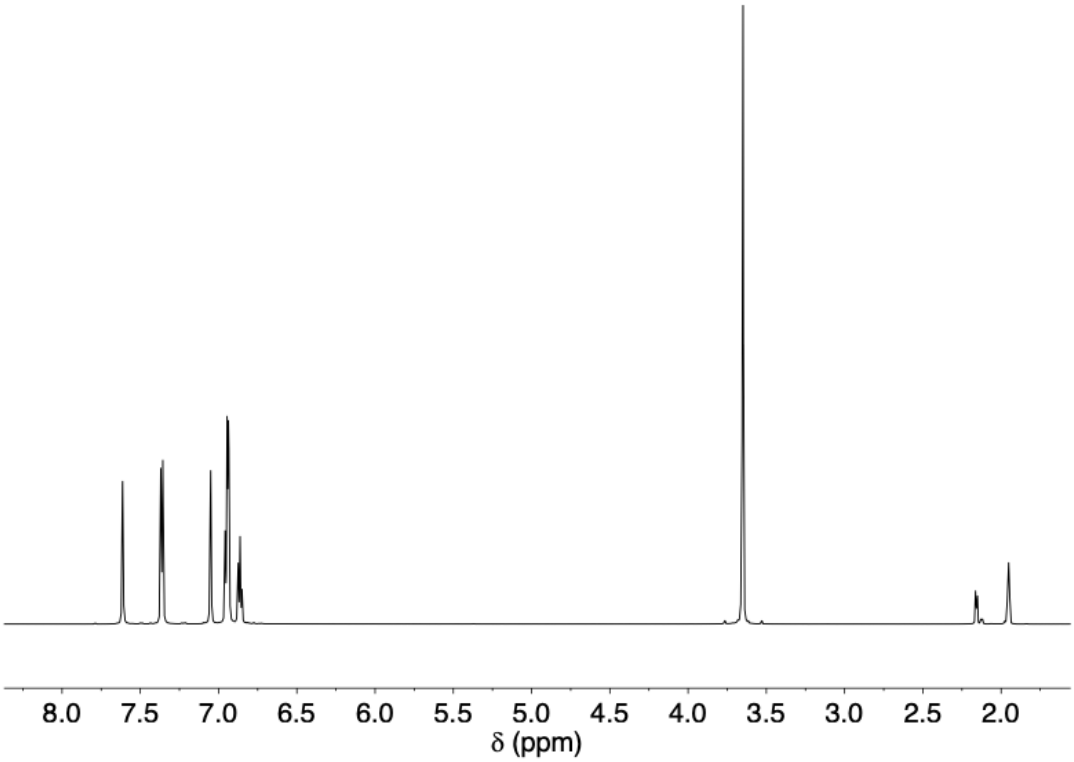

Fig. S4 Solution ^{1}H NMR of **4** in acetonitrile-d_3.

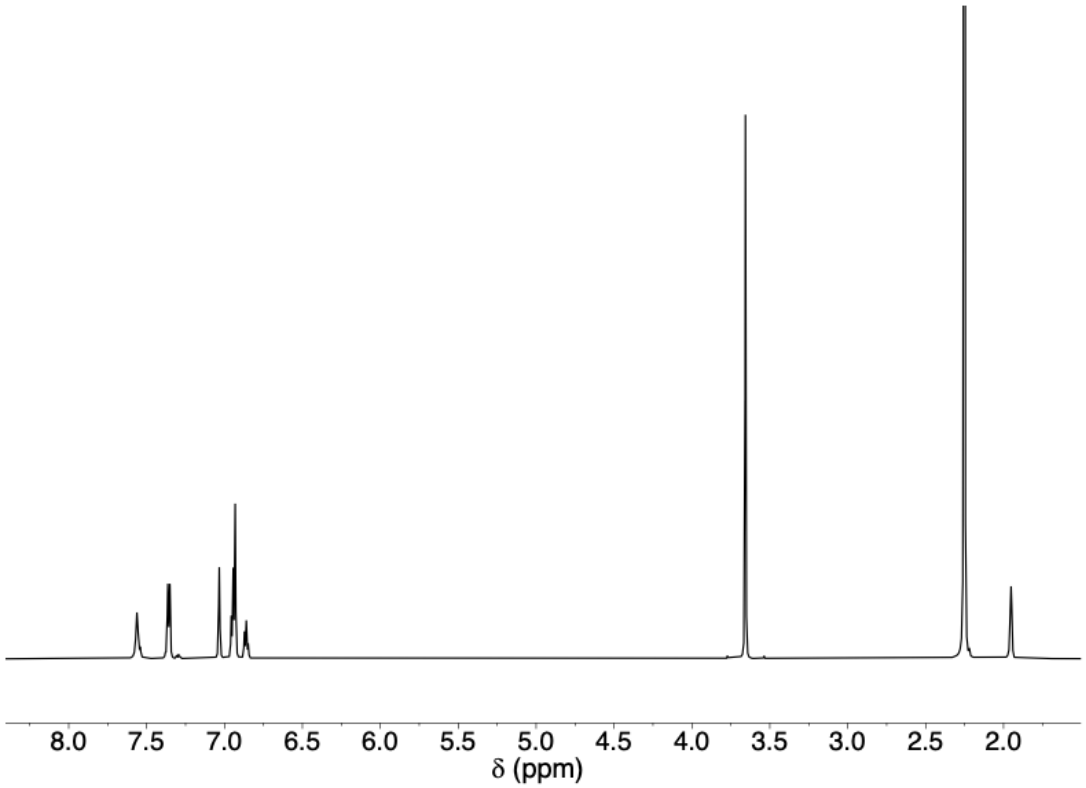

Fig. S5 Solution ^{1}H NMR of **4** in acetonitrile-d_3 after being exposed to air for 7 d (21 ˚C, 20-90 %RH). The peak at 2.25 ppm corresponds to H_2O.

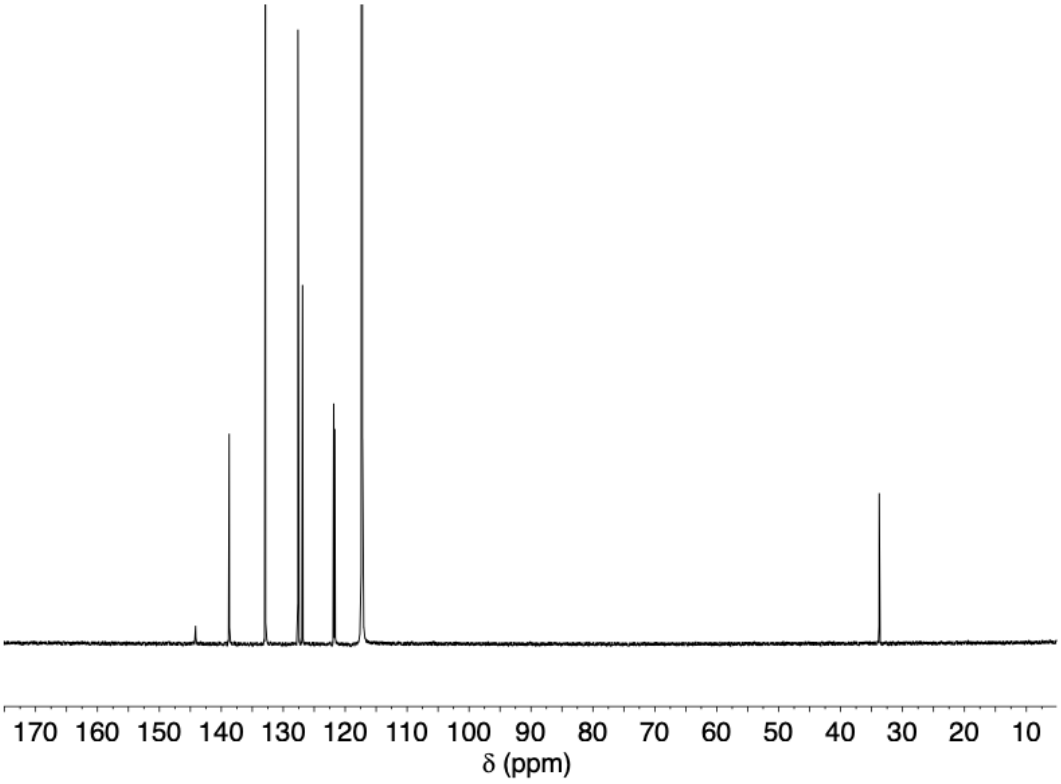

Fig. S6 Solution ^{13}C NMR of **4** in acetonitrile-d_3.

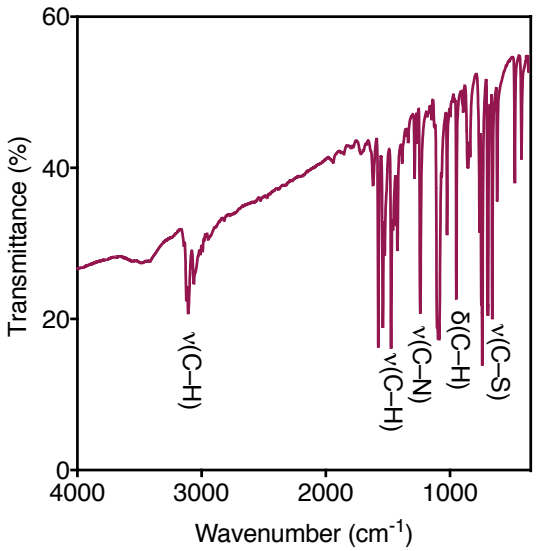

Fig. S7 FT-IR spectrum of **4** (KBr).

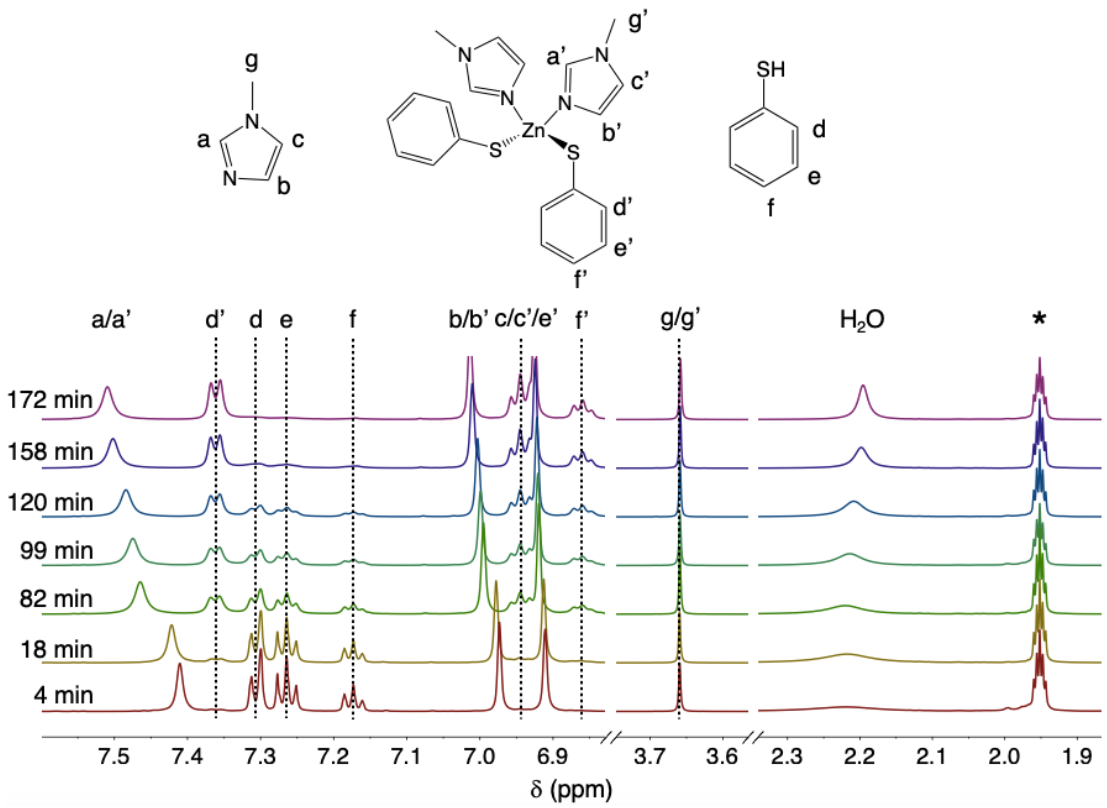

Fig. S8 Stacked room-temperature solution ^{1}H NMR spectra in acetonitrile-d_3 of the aromatic region, methyl, and H_2O peaks for aliquots taken as a function of time from the dissolution of ZnO with MeIm (3 eq) and thiophenol (2.4 eq) at 75 °C. Acetonitrile-d_2 is labeled as *.

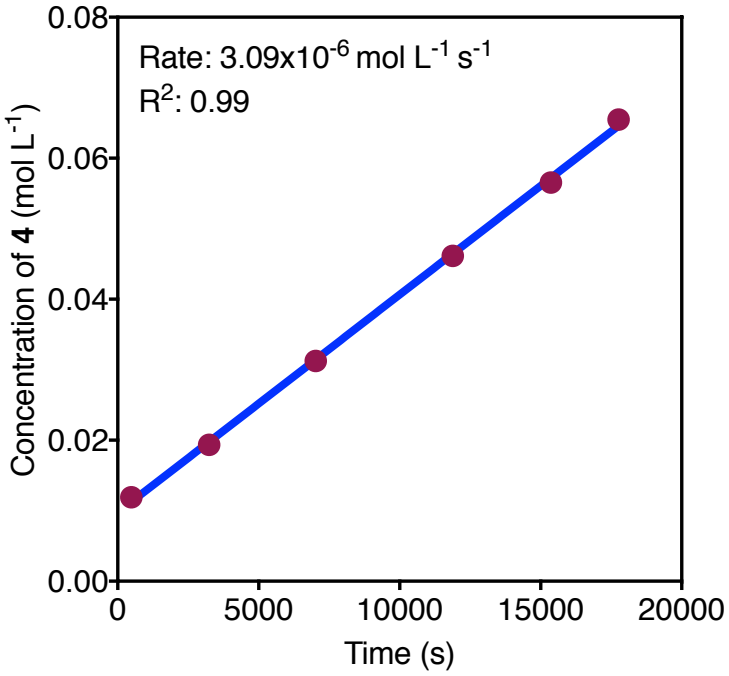

Fig. S9 Plot of ZnO dissolution at 30 °C with concentration of **4** in solution *vs.* time. Dissolution was performed with 2.4 eq thiophenol and 3 equiv MeIm relative to ZnO. Zero-order dissolution kinetics are seen through completion of dissolution.

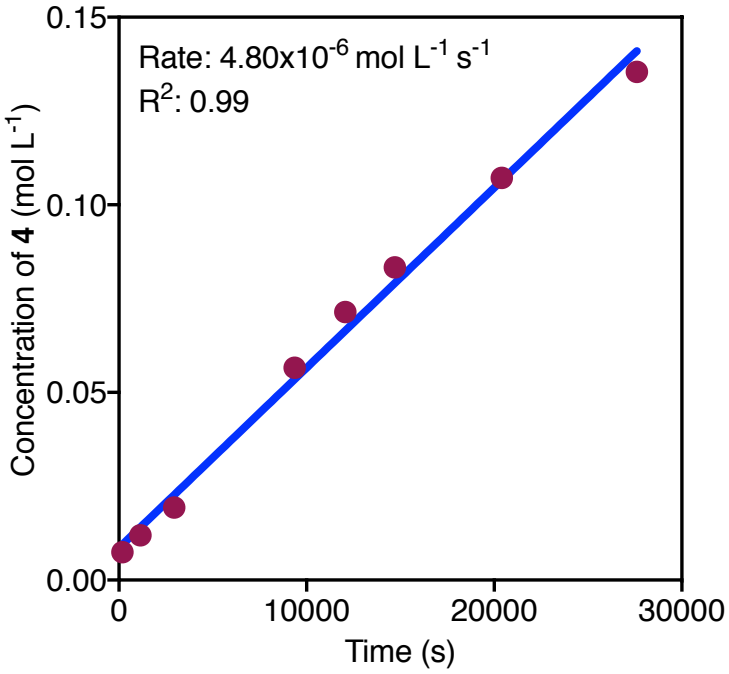

Fig. S10 Plot of ZnO dissolution at 40 °C with concentration of **4** in solution *vs.* time. Dissolution was performed with 2.4 eq thiophenol and 3 equiv MeIm relative to ZnO. Zero-order dissolution kinetics are seen through completion of dissolution.

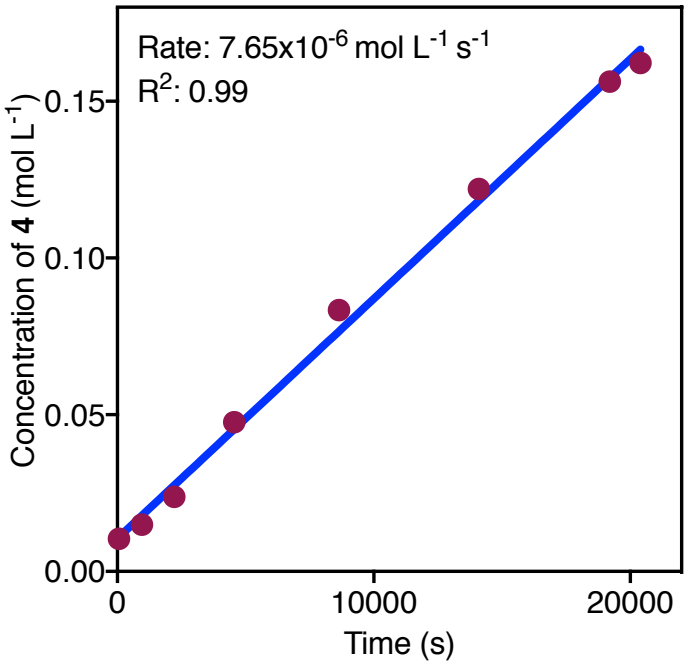

Fig. S11 Plot of ZnO dissolution at 55 °C with concentration of **4** in solution *vs.* time. Dissolution was performed with 2.4 eq thiophenol and 3 equiv MeIm relative to ZnO. Zero-order dissolution kinetics are seen through completion of dissolution.

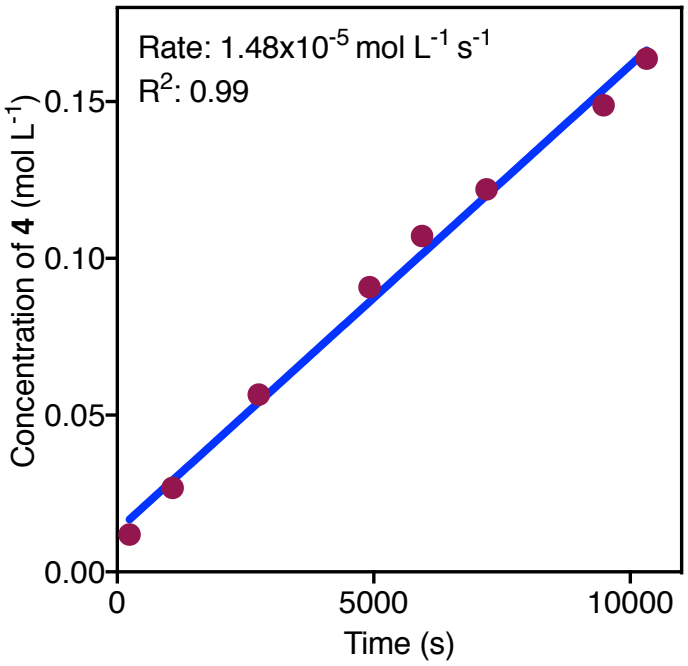

Fig. S12 Plot of ZnO dissolution at 75 °C with concentration of **4** in solution *vs.* time. Dissolution was performed with 2.4 eq thiophenol and 3 equiv MeIm relative to ZnO. Zero-order dissolution kinetics are seen through completion of dissolution.

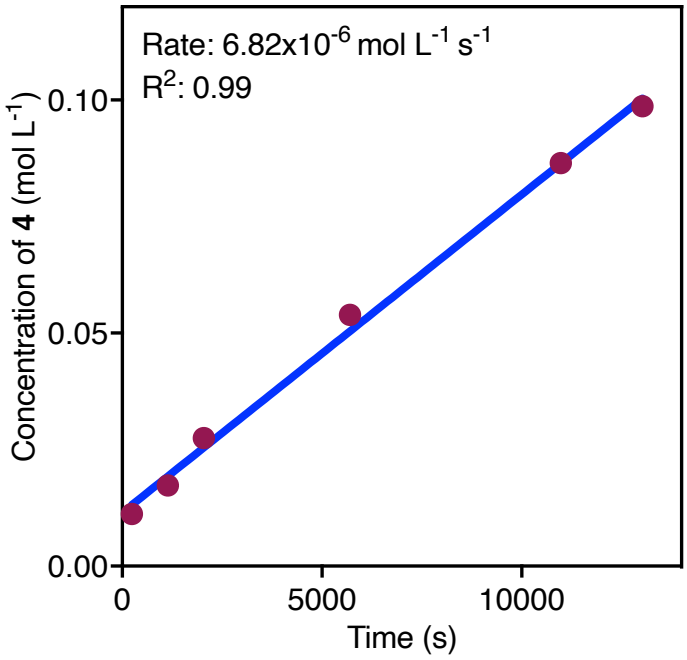

Fig. S13 Plot of ZnO dissolution at 75 °C with concentration of **4** in solution *vs.* time. Dissolution was performed with stoichiometric thiophenol (2.05 eq) and MeIm (2.05 eq) relative to ZnO. Zero-order dissolution kinetics are seen through completion of dissolution.

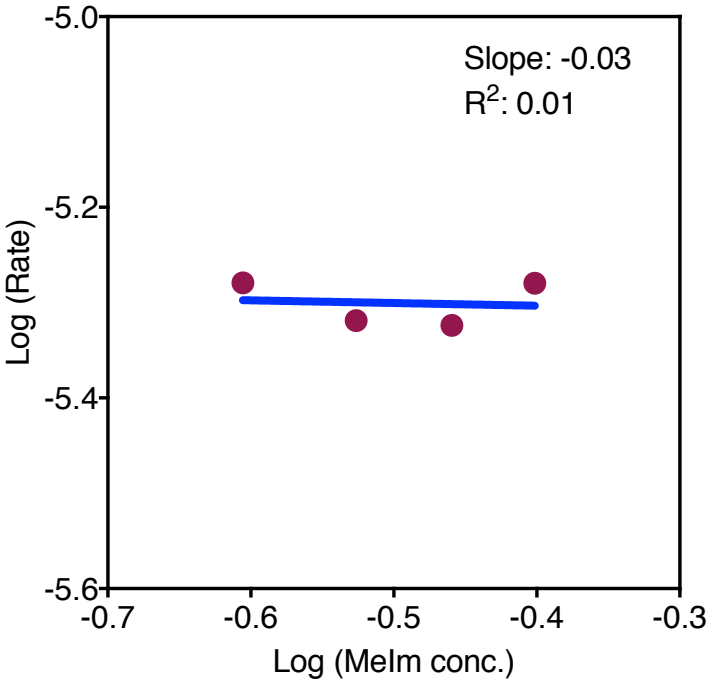

Fig. S14 Log-log plot of rate of ZnO dissolution *vs.* MeIm concentration at 40 °C, where MeIm is present in excess (from 2.4-4.0 eq relative to ZnO). Zero-order dissolution kinetics are seen through completion of dissolution.

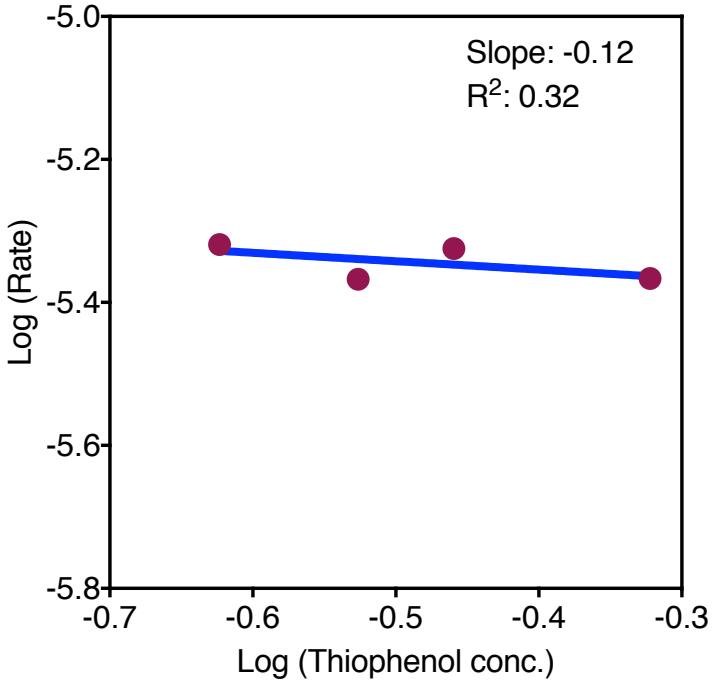

Fig. S15 Log-log plot of rate of ZnO dissolution *vs.* thiophenol concentration at 40°C, where thiophenol is present in excess (from 2.4-4.8 eq relative to ZnO). Zero-order dissolution kinetics are seen through completion of dissolution.

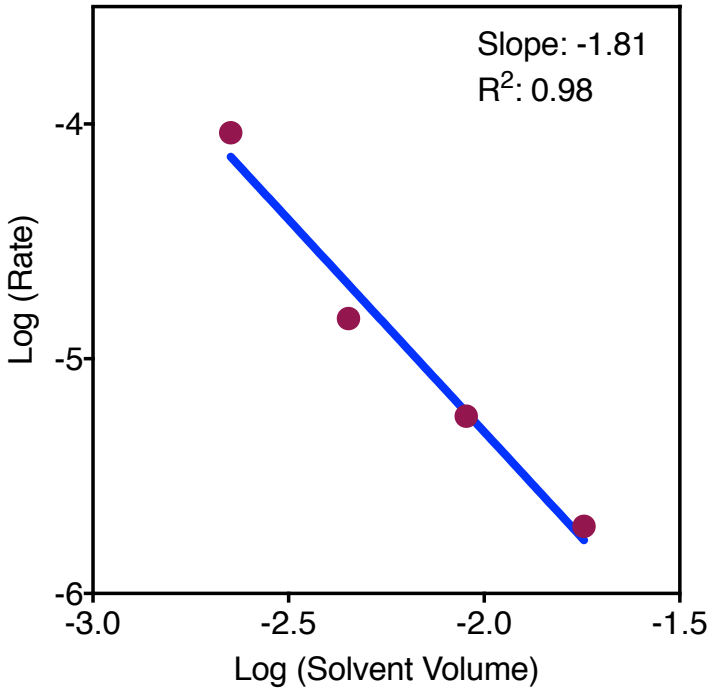

Fig. S16 Log-log plot of solvent volume *vs.* rate of ZnO dissolution (75 °C).

Rate Law and Derivation

We have observed two kinetic regimes for dissolution of ZnO under the reported conditions. In cases where ligands are abundant, rate conforms to a Michealis-Menten saturation kinetics model, where the apparent catalyst models a reactive site on the ZnO surface. In cases where ligand is scarce, the saturation model loses relevance, and we treat the system with a steady-state approximation.

Key: **Ref** = ZnO surface; **1** = binding of thiophenol (with concomitant Zn–OH formation) to ZnO; **2** = binding of MeIm to **1**, as labeled in the main text, **Fig. 4**.

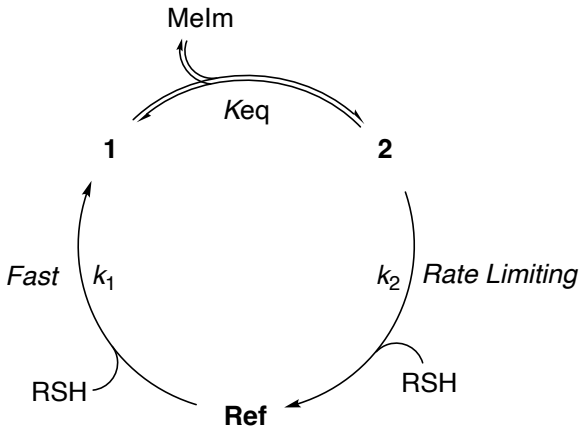

Fig. S17 Proposed cycle for product evolution from a surface reactive site. Note that a second equivalent of MeIm enters the reaction in the conversion of **3** to **4**, but this step is kinetically invisible, so it does not enter the model.

Derivation of the steady-state rate law.

Rate definition: $Rate = -\frac{d}{dt}[\mathbf{2}] = k_2[\mathbf{2}][\mathrm{RSH}]$

Equilibrium between **1** and **2**: $\frac{[\mathbf{1}]}{[\mathbf{2}]} = \frac{1}{K_{eq}[\mathrm{MeIm}]}$

Steady-state approximation on [**Ref**]: $k_2[\mathbf{2}][\mathrm{RSH}] = k_1[\mathbf{Ref}][\mathrm{RSH}]$

$$\frac{[\mathbf{Ref}]}{[\mathbf{2}]} = \frac{k_2}{k_1}$$

Total reactive sites $[\mathrm{Zn}]_{\mathrm{tot}}$: $[\mathrm{Zn}]_{\mathrm{tot}} = [\mathbf{Ref}] + [\mathbf{1}] + [\mathbf{2}] = [\mathbf{2}][\frac{k_2}{k_1} + \frac{1}{K_{\mathrm{eq}}[\mathrm{MeIm}]} + 1]$

Three-term rate law: $Rate = \frac{k_2[\mathrm{Zn}]_{\mathrm{tot}}[\mathrm{RSH}]}{[\frac{k_2}{k_1} + \frac{1}{K_{\mathrm{eq}}[\mathrm{MeIm}]} + 1]}$

Assuming that $k_1 >> k_2$ (*i.e.*, conversion of **2** is rate limiting):

$$Rate = \frac{k_2[\mathrm{Zn}]_{\mathrm{tot}}[\mathrm{RSH}]}{\left[\frac{1}{K_{\mathrm{eq}}[\mathrm{MeIm}]}+1\right]}$$

This rate law accounts for first order dependance on thiol and partial positive dependance on methylimidazole, as observed when the reaction is diluted.

Assuming that K_{eq}[Im] << 1 (*i.e.*, [**1**] is more abundant than [**2**]):

$$Rate = k_2[\mathrm{Zn}]_{\mathrm{tot}}[\mathrm{RSH}][\mathrm{MeIm}]$$

This assumption is not reasonable in scarce ligand conditions, which is consistent with observation of only partial order on [MeIm] in a dilution experiment.

Table S1. Eyring data for the dissolution of ZnO at various temperatures. Error statistics for $\Delta H^{\ddagger}$ and $\Delta S^{\ddagger}$ derived from the analysis performed in reference 1.

Temperature (°C)	Rate (mol L^{-1} s^{-1})	Error in rate (mol L^{-1} s^{-1})	$R\ln(k/T) - R\ln(k_B/h)$ (J/mol•K)	$\Delta H^{\ddagger}$ error (J/mol•K)[1]	$\Delta S^{\ddagger}$ error (J/mol•K)[1]
30	3.09×10^{-6}	4.53×10^{-8}	-350.54	0.48	1.25
40	4.80×10^{-6}	1.61×10^{-7}	-347.14	1.01	2.86
55	7.65×10^{-6}	1.99×10^{-7}	-343.66	0.79	2.23
75	1.48×10^{-6}	4.67×10^{-7}	-338.64	0.95	2.68

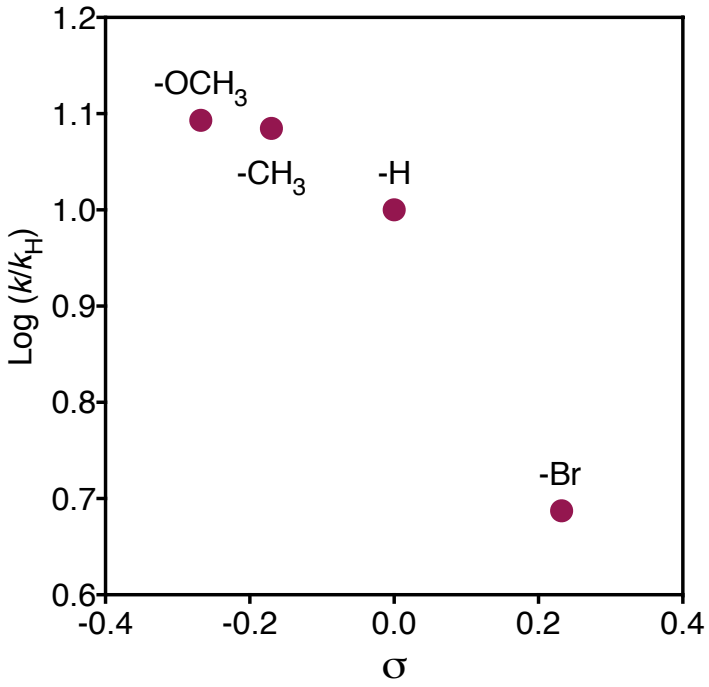

Fig. S18 Hammett plot corresponding to ZnO dissolution reaction at 40 °C with 2.4 eq of *para*-substituted thiophenol and 3 eq of MeIm with respect to ZnO.

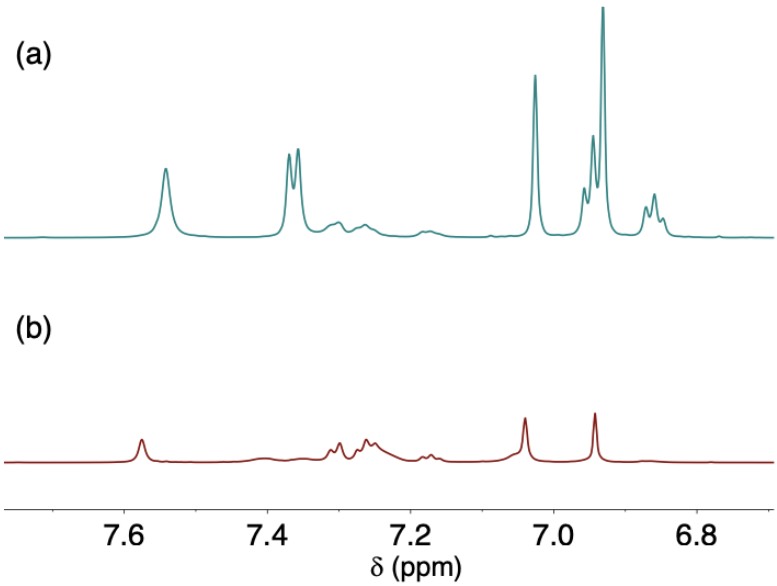

Fig. S19 (a) Solution ^{1}H NMR spectra of the aromatic region of a fully dissolved reaction mixture of ZnO with MeIm (3 eq) and thiophenol (2.4 eq) in acetonitrile-d_3. This reaction proceeds readily to form **4**. (b) Upon addition of a more electron rich 4-bromothiophenol at 75 °C, the displacement of the thiophenolate ligands for 4-bromothiophenolate ligands with the formation of $Zn(SPhBr)_2(MeIm)_2$ by the appearance of the resonances at δ = 7.24 and 7.06 ppm and the concomitant disappearance of thiophenolate protons at δ = 7.36, 6.95 and 6.86 ppm. We see the relative intensities of free thiophenol also increase at δ = 7.30, 7.26 and 7.17 ppm after the addition of 4-bromothiophenol.

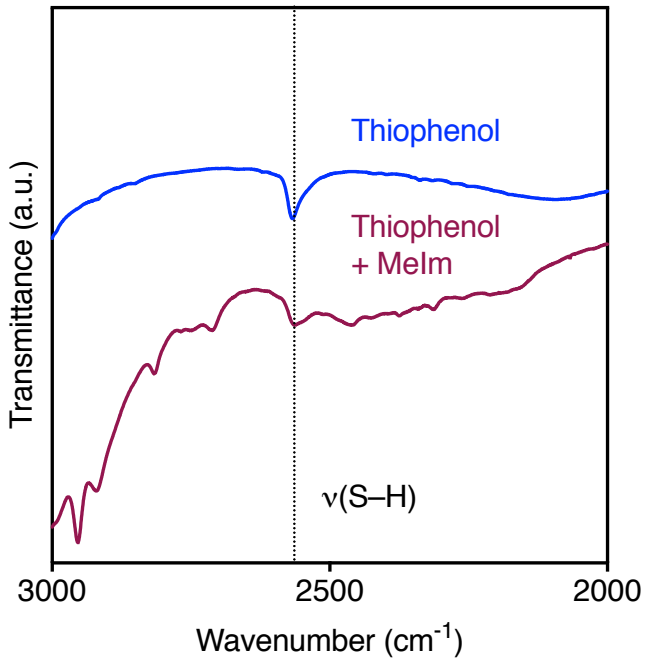

Fig. S20 FT-IR spectra of the sulfhydryl region showing the ν(S–H) stretch of thiophenol before and after addition of MeIm in acetonitrile (NaCl plates).

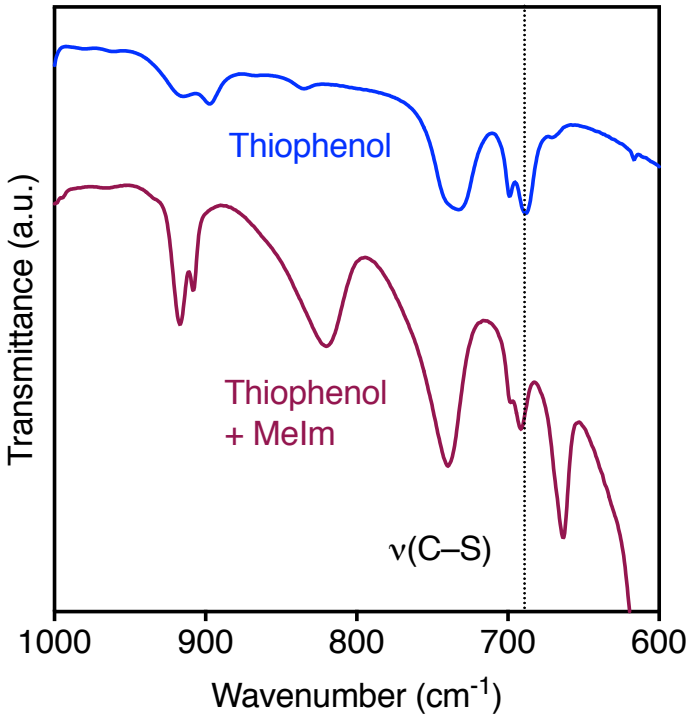

Fig. S21 FT-IR spectra showing the ν(C–S) stretch of thiophenol before and after addition of MeIm in acetonitrile (NaCl plates).

Table S2. Room-temperature electrolytic conductivity measurements in acetonitrile under flowing nitrogen between two Pt wires. The measurements were run in triplicate for accuracy at 100 mV applied potential.

Sample	Voltage (V)	Current (A)
MeIm	0.1	5.98×10^{-10}
MeIm	0.1	5.66×10^{-10}
MeIm	0.1	7.55×10^{-10}
MeIm titrated w/ thiophenol	0.1	6.03×10^{-8}
MeIm titrated w/ thiophenol	0.1	5.39×10^{-8}
MeIm titrated w/ thiophenol	0.1	5.23×10^{-8}

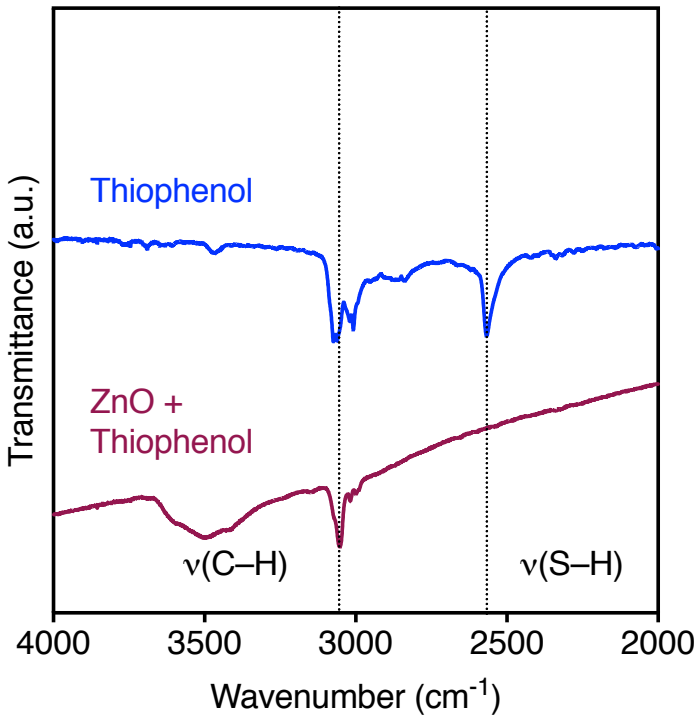

Fig. S22 FT-IR spectra showing the ν(C–H) and ν(S–H) stretching region (KBr). ZnO was mixed with thiophenol at 75 °C, washed and dried under high vacuum overnight at room temperature.

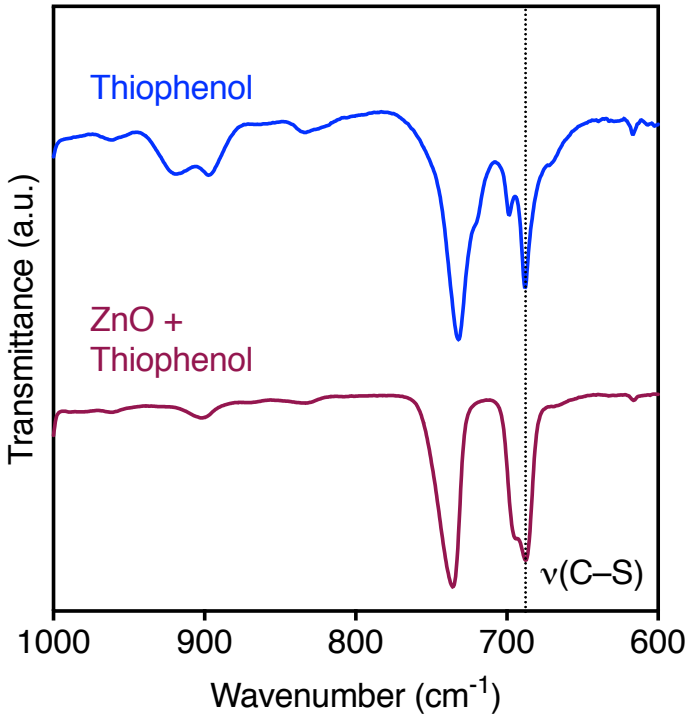

Fig. S23 FT-IR spectra showing the ν(S–C) stretching region (KBr). ZnO was mixed with thiophenol at 75 °C, washed and dried under high vacuum overnight at room temperature.

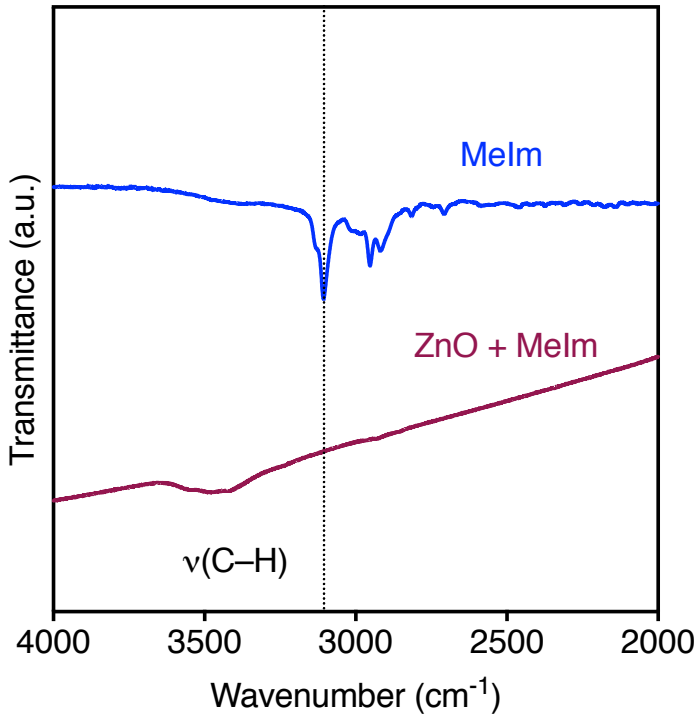

Fig. S24 FT-IR spectra showing the ν(C–H) stretching region (KBr). ZnO was mixed with MeIm at 75 °C, washed and dried under high vacuum overnight at room temperature.

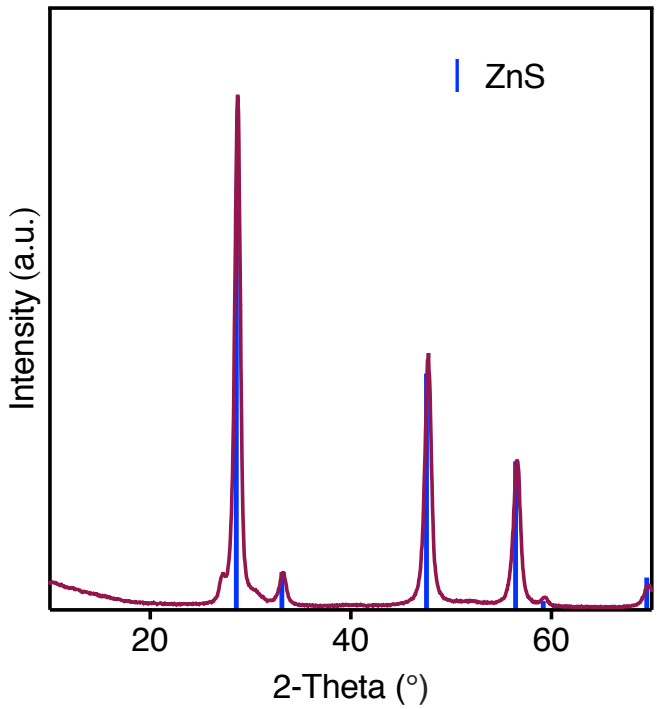

Fig. S25 Powder XRD pattern of polycrystalline ZnS powder starting material (99.99%, Sigma-Aldrich) indexed to the sphalerite crystal structure.

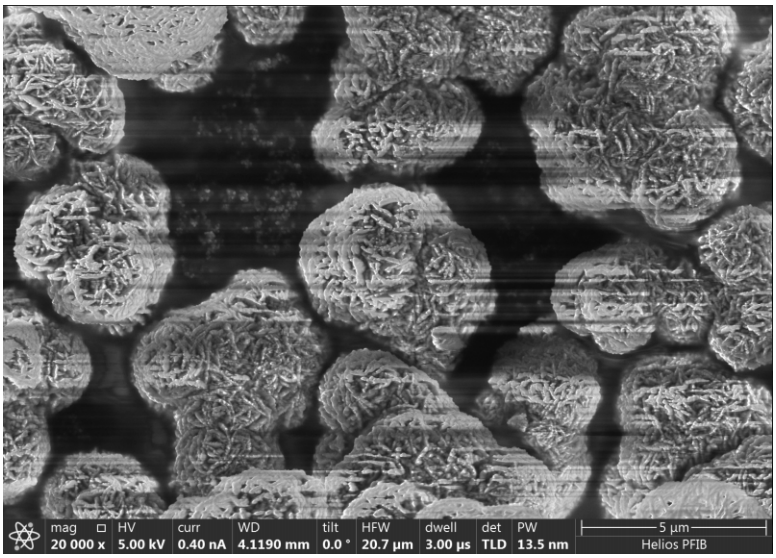

Fig. S26 SEM micrograph of polycrystalline ZnS powder starting material (99.99%, Sigma-Aldrich).

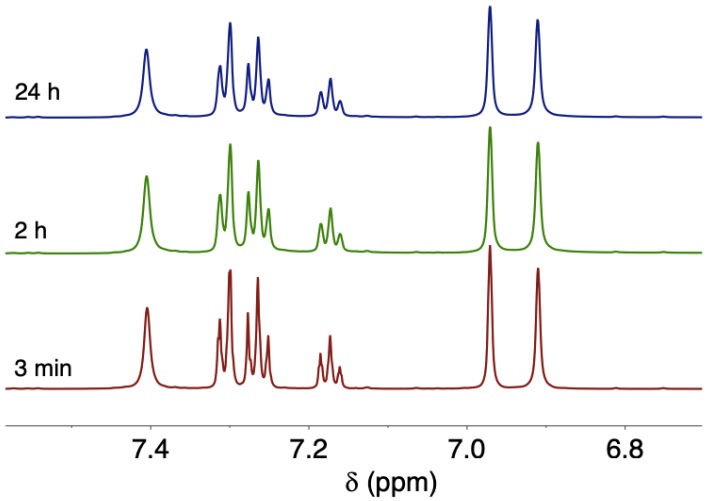

Fig. S27 ^{1}H NMR spectra of the aromatic region of aliquots from the reaction of ZnS with MeIm (3 eq) and thiophenol (2.4 eq) in acetonitrile-d_3 at 75 °C demonstrating lack of dissolution.

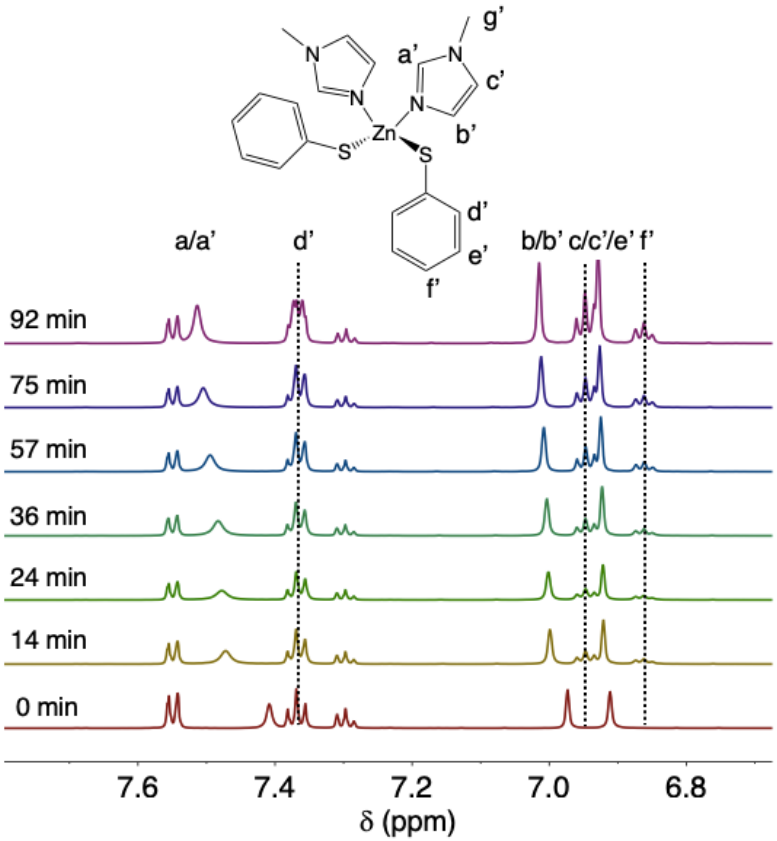

Fig. S28 Stacked ^{1}H NMR spectra of the aromatic region of aliquots from the dissolution of Zn metal with MeIm (3 eq) and diphenyl disulfide (2.4 eq) in acetonitrile-d_3 at 75 °C. This reaction readily proceeds to form **4**, as evidenced by the appearance of the bound thiophenolate protons at δ = 7.36, 6.95, 6.86 ppm. Resonances at δ = 7.56, 7.38 and 7.30 represent aromatic protons of diphenyl disulfide.

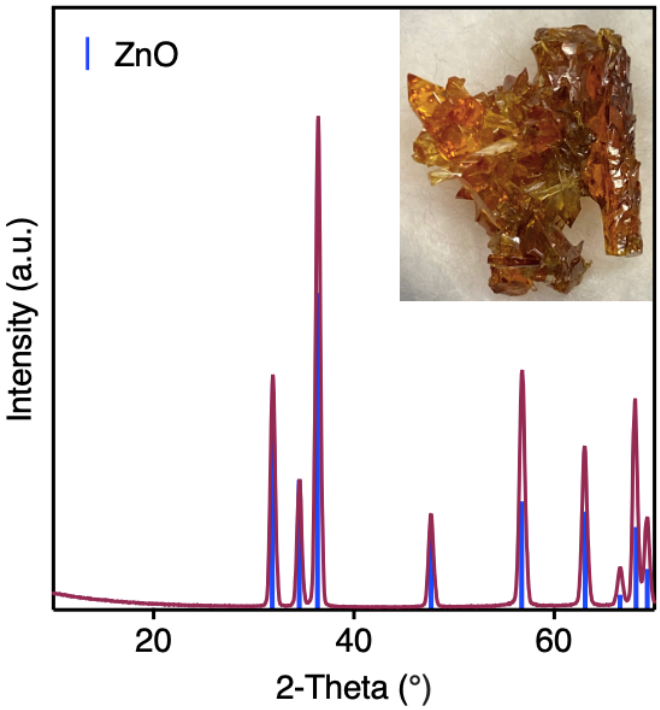

Fig. S29 Powder XRD pattern of natural zincite mineral powder indexed to the wurtzite crystal structure. A photograph of the as-received mineral sample is shown as the inset.

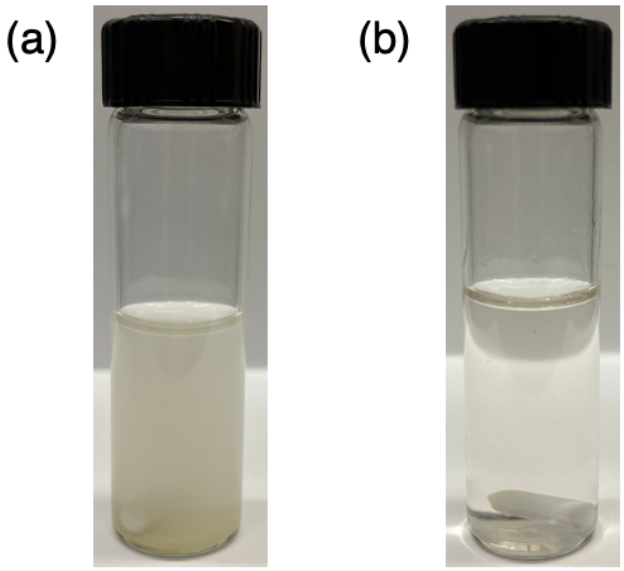

Fig. S30 Representative photographs of natural zincite dissolution in MeIm and acetonitrile (a) before thiophenol addition and (b) after thiophenol addition and full dissolution.

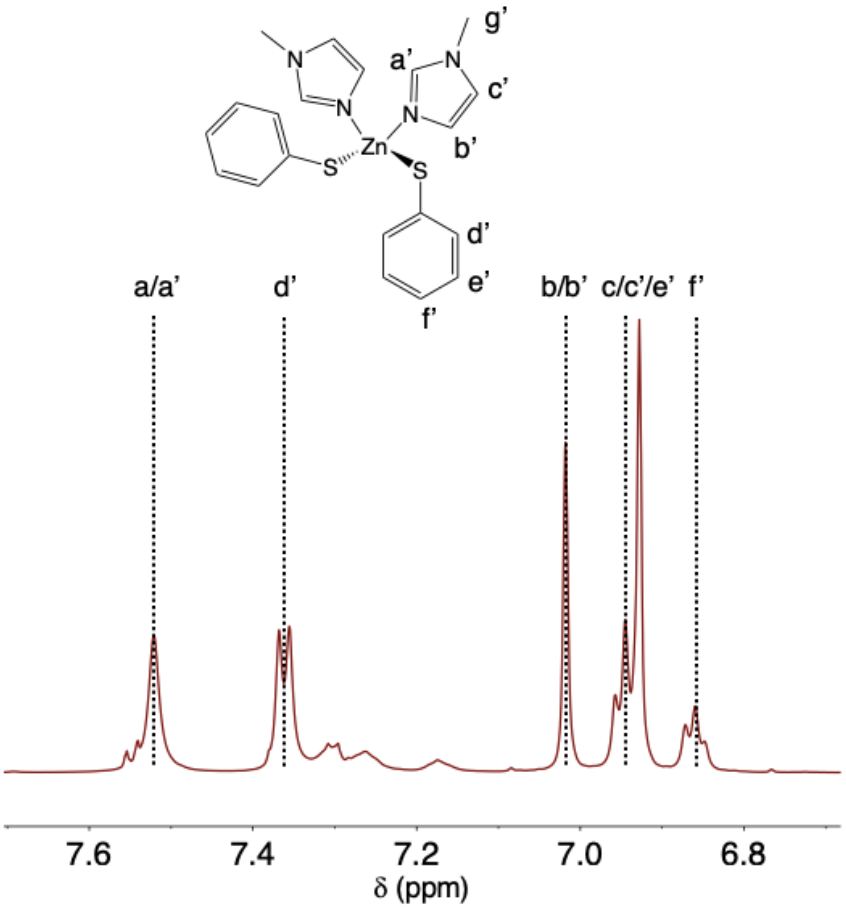

Fig. S31 ^{1}H NMR spectrum of the aromatic region from the dissolution of natural zincite mineral with MeIm (3 eq) and thiophenol (2.4 eq) in acetonitrile-d_3 at 75 °C after full dissolution. This reaction readily proceeds to form **4**, as evidenced by the appearance of the bound thiophenolate protons at δ = 7.36, 6.95, 6.86 ppm.

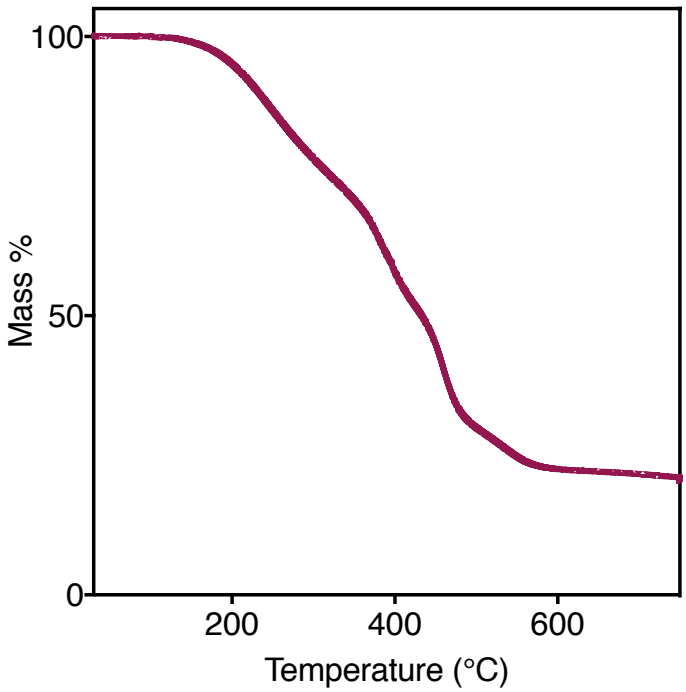

Fig. S32 TGA trace of the thermal decomposition of **4**.

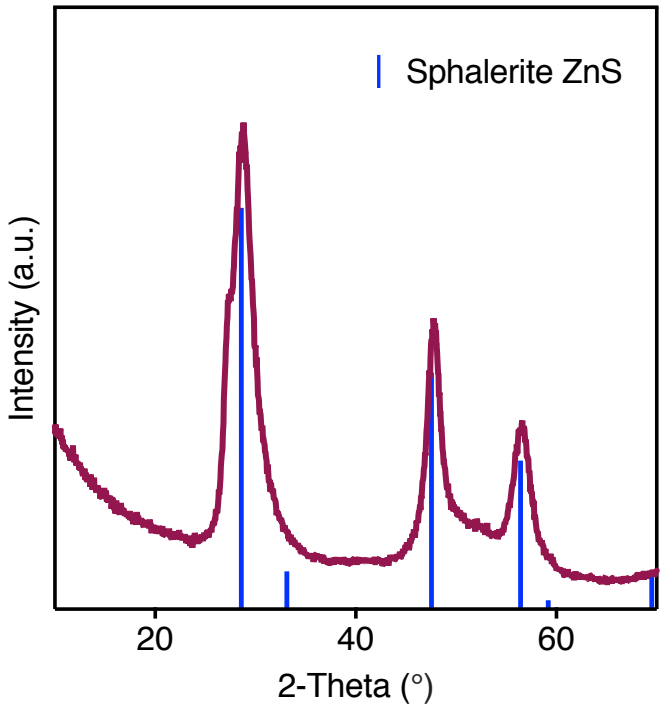

Fig. S33 Powder XRD pattern of the thermal decomposition product of **4** annealed at 600 °C for 30 h, indexed to cubic sphalerite ZnS.

References

1. T. J. Williams, A. D. Kershaw, V. Li and X. Wu, *J. Chem. Educ.*, 2011, **88**, 665−669.